Cell Research (2012) 22:1356-1373.

www.nature.com/cr

ORIGINAL ARTICLE

Differential secretome analysis reveals CST6 as a suppressor of breast cancer bone metastasis

Lei Jin[1, *], Yan Zhang[2, *], Hui Li[1], Ling Yao[2], Da Fu[1], Xuebiao Yao[3], Lisa X Xu[2], Xiaofang Hu[2], Guohong Hu[1]

[1]The Key Laboratory of Stem Cell Biology, Institute of Health Sciences, Shanghai Institutes for Biological Sciences, Chinese Academy of Sciences & Shanghai Jiao Tong University School of Medicine, 225 South Chongqing Rd, Shanghai 200025, China; [2]School of Biomedical Engineering and Med-X Research Institute, Shanghai Jiao Tong University, 1954 Huashan Rd, Shanghai 200030, China; [3]Anhui Key Laboratory of Cellular Dynamics & Chemical Biology, University of Science & Technology of China, Hefei, Anhui 230027, China

Bone metastasis is a frequent complication of breast cancer and a common cause of morbidity and mortality from the disease. During metastasis secreted proteins play crucial roles in the interactions between cancer cells and host stroma. To characterize the secreted proteins that are associated with breast cancer bone metastasis, we preformed a label-free proteomic analysis to compare the secretomes of four MDA-MB-231 (MDA231) derivative cell lines with varied capacities of bone metastasis. A total of 128 proteins were found to be consistently up-/down-regulated in the conditioned medium of bone-tropic cancer cells. The enriched molecular functions of the altered proteins included receptor binding and peptidase inhibition. Through additional transcriptomic analyses of breast cancer cells, we selected cystatin E/M (CST6), a cysteine protease inhibitor down-regulated in bone-metastatic cells, for further functional studies. Our results showed that CST6 suppressed the proliferation, colony formation, migration and invasion of breast cancer cells. The suppressive function against cancer cell motility was carried out by cancer cell-derived soluble CST6. More importantly, ectopic expression of *CST6* in cancer cells rescued mice from overt osteolytic metastasis and deaths in the animal study, while *CST6* knockdown markedly enhanced cancer cell bone metastasis and shortened animal survival. Overall, our study provided a systemic secretome analysis of breast cancer bone tropism and established secreted CST6 as a *bona fide* suppressor of breast cancer osteolytic metastasis.

***Keywords*:** breast cancer; bone metastasis; secretome; proteomics; cystatin; CST6

Cell Research (2012) **22**:1356-1373. doi:10.1038/cr.2012.90; published online 12 June 2012

Introduction

Breast cancer is the most frequent type of malignancy and the leading cause of cancer deaths of women in both developed and developing countries [1]. The majority of patient deaths are due to the growth of disseminated tumor cells in distant organs, i.e., metastasis. Among all the human organs, bone is the most favorite target of metastatic breast cancer cells [2]. Bone metastasis affects over 70% of the patients with advanced diseases, leading to intractable pain, bone fragility, nerve compression, hypercalcaemia, leukoerythroblastic anaemia and eventually patient demise [3]. Therefore, it is a pressing need to uncover the molecular underpinning of bone metastasis in order to develop effective therapies for breast cancer.

The development of tumor metastasis tumors depends on the mutual communication between cancer cells and their stromal milieu. The molecular interactions of metastasizing tumor cells with host cells and extracellular matrix (ECM) enable the tumor cells to modify the stromal components and turn them into accomplices for ECM remodeling, immune suppression, host tissue destruction and angiogenesis, all of which are essential for metastasis [4]. It is generally conceived that tumor-derived secreted factors play critical roles in this abetting process [5, 6]. A plethora of secreted proteins have been

*These two authors contributed equally to this work.
Correspondence: Guohong Hu[a], Xiaofang Hu[b], Lisa X Xu[c]
[a]Tel: 86-21-63844516
E-mail: ghhu@sibs.ac.cn
[b]E-mail: xfhu@sjtu.edu.cn
[c]E-mail: lisaxu@sjtu.edu.cn
Received 25 December 2011; revised 18 March 2012; accepted 4 April 2012; published online 12 June 2012

shown to direct the cell-cell and cell-microenvironment interactions that drive cancer spreading. For example, cytokines are often found to mediate the directed migration of cancer cells during metastasis [7], and induce the infiltration of inflammatory cells with pro-tumor characteristics in advanced-stage carcinoma [8]. Proteinases represent another important class of environmental molecules that regulate ECM remodeling, cancer cell invasion and cytokine mobilization [9, 10]. Some metalloproteinases, such as MMP1 and MMP2, are well known for their roles of enhancing distant metastasis through their proteolytic activities [9]. In addition, growth factors are widely reported to function in various metastasis-associated processes including cancer cell epithelial-mesenchymal transition, migration, invasion, survival and angiogenesis [11]. Tumor-secreted proteins cannot only remodel the local microenvironment for tumor spreading, but also manipulate distant tissues to facilitate future metastasis. They reach target organs ahead of metastasis cancer cells and adapt the foreign tissues into a tumor-friendly environment that is called "metastasis niche" [12]. Overall, cancer cell secretome is a rich reservoir of biomarkers of cancer progression and molecular targets of cancer therapeutics, and thus is a topic of great interest for cancer research [5, 13].

Proteomics provides a powerful way to identify and compare secreted proteins in different cell lines or tissues. With recent advance of proteomic techniques, an increasing number of studies have characterized the cancer cell secretomes associated with cancer initiation, progression and chemoresistance [14-20], which have greatly enriched our understanding of the roles of secreted proteins in cancer, and provided a good resource of cancer-specific biomarkers with potentials of therapeutic application. However, fewer studies have been focused on proteomic analyses of cancer secretomes related to metastasis. Among the pioneering work of metastasis secretome analyses, Kreunin *et al*. [21] profiled the proteins in the conditional medium (CM) of a pair of M DA-MB-435 derivative cell lines with different metastatic phenotypes. Several proteins such as OPN and ECM1 were found to be enriched in the medium of metastatic cells. Rocco *et al*. [22]performed secretome profiling of several cancer cell lines from different metastases of a melanoma patient and found that a list of matricellular proteins including SPARC, OPN and ECM1 were associated with melanoma metastasis. Mbeunkui *et al.*[23] analyzed the secretomes of the MCF10 cell line series, a model of breast cancer progression, and identified five proteins highly secreted by the more aggressive cells. Similarly, Xue *et al.* [24] studied the secreted proteins of the colorectal cancer cell line SW480 and its metastatic subline SW620. Among the differentially expressed proteins, TFF3 and GDF15 were further shown to be correlated with lymph node metastasis of clinical samples. Several more studies reported differentially secreted proteins associated with metastasis of melanoma, lung cancer and ovarian cancer [25-28]. However, so far systemic analyses of tumor-derived soluble proteins correlated with bone metastasis have been lacking, and thus the nature of changes in protein secretion leading to this frequent complication of cancer remains elusive.

In the present work, we performed liquid chromatography-tandem mass spectrometry (LC-MS/MS)-based secretome profiling for four derivative lines of MD231 with varied tendencies of bone metastasis. A total of 2 069 proteins were identified in the CM of cancer cells, among which 128 species displayed differential secretion levels in these cell lines. Notably, proteinase inhibitors were significantly enriched in the regulated proteins, indicating a critical role of proteinase activities in the tumor environment during breast cancer bone metastasis. In the functional validation, we showed that one of the proteinase inhibitors, CST6, suppressed the migration, invasion and *in vivo* bone metastasis of breast cancer cells. Furthermore, CST6 played the metastasis-inhibiting role in its soluble form, supporting that it is a secreted suppressor of metastasis.

Results

Secretome analysis of breast cancer bone metastasis

In order to characterize the secreted proteins associated with breast cancer bone metastasis, we took advantage of the MDA231 derivative cell line model. By single cell progeny (SCP) cloning, Kang *et al*. [29] established a series of sublines from MDA231, a cell line obtained from the pleural fluid of a patient with metastatic breast cancer. Among the MDA231 derivatives, SCP2 and SCP46 developed osteolytic bone metastasis rapidly when injected intracardiacally into immunodeficient mice, while SCP4 and SCP6 displayed much weaker metastasis capabilities. Since then this cell line model has been widely used to study the molecular and stromal mechanisms of breast cancer bone metastasis [30-34]. We performed secretome profiling of SCP4, SCP6, SCP2 and SCP46 cells with LC-MS/MS following one-dimensional gel electrophoresis and in-gel digestion (1D GeLC-MS/MS). In the workflow elaborated in Figure 1, serum-free CM of the four cell lines were collected individually, and three independent technical replicates of each line were analyzed. The proteomic analyses identified 1 445, 1 527, 1 478 and 1 423 proteins in the CM of each cell line, and 2 069 proteins collectively. Of them, 1 029, 1 035, 975 and

998 proteins were detected in all the three replicates of each cell line, accounting for 71.2%, 67.8%, 66.0% and 70.1% of the identified proteins (Figure 2A). In general, we achieved a technical reproducibility of 80.0% ± 3.1% for any two replicates and 68.8% ± 2.3% for three replicates.

We further analyzed the subcellular localization of the identified proteins. In the CM of the four cell lines, 25.9% - 28.5% of the identified proteins were known to be secreted or predicted to be secreted, and 38.9% - 39.4% were categorized as plasma membrane proteins, together accounting for 65.3% - 67.7% of the total (Figure 2B). The remaining proteins were either intracellular (29.7% - 31.6%) or unknown (2.6% - 3.1%). The spectral counts of protein in the 1D GeLC-MS/MS analysis are indicative of protein abundance. Therefore, we performed subcellular localization analysis of the identified proteins weighted with their corresponding spectral counts as well, and found that 42.3% - 49.0% of the spectral counts were attributed to secreted proteins (Figure 2C). The fractions of secreted proteins weighted by spectral counts were significantly higher than the unweighted fractions, suggesting that these proteins were more abundantly detected in the CM. Indeed, the average spectral counts of secreted proteins were in general more than 2 folds higher than those of other proteins in the four cell lines ($P < 1 \times 10^{-5}$).

Identification of bone metastasis-associated proteins

Next, we compared the secretomes of these cell lines to search for the proteins associated with bone metastasis, with an emphasis on secreted proteins. As shown in Supplementary information, Figure S1, 1 761 proteins were detected in the CM of weakly metastatic cells SCP4 and SCP6, and 1 708 proteins detected in that of bone-tropic cells SCP2 and SCP46. Subcellular localization analysis identified 468 and 473 secreted proteins in each group. We compared the abundance of these proteins in the CM of two cell groups and found that 128 proteins were differentially secreted with spectral count fold changes > 2 and Student's *t*-test *P* values < 0.05, among which 69 proteins were up-regulated and 59 down-regulated in metastatic cells (Supplementary information, Tables S1 and S2).

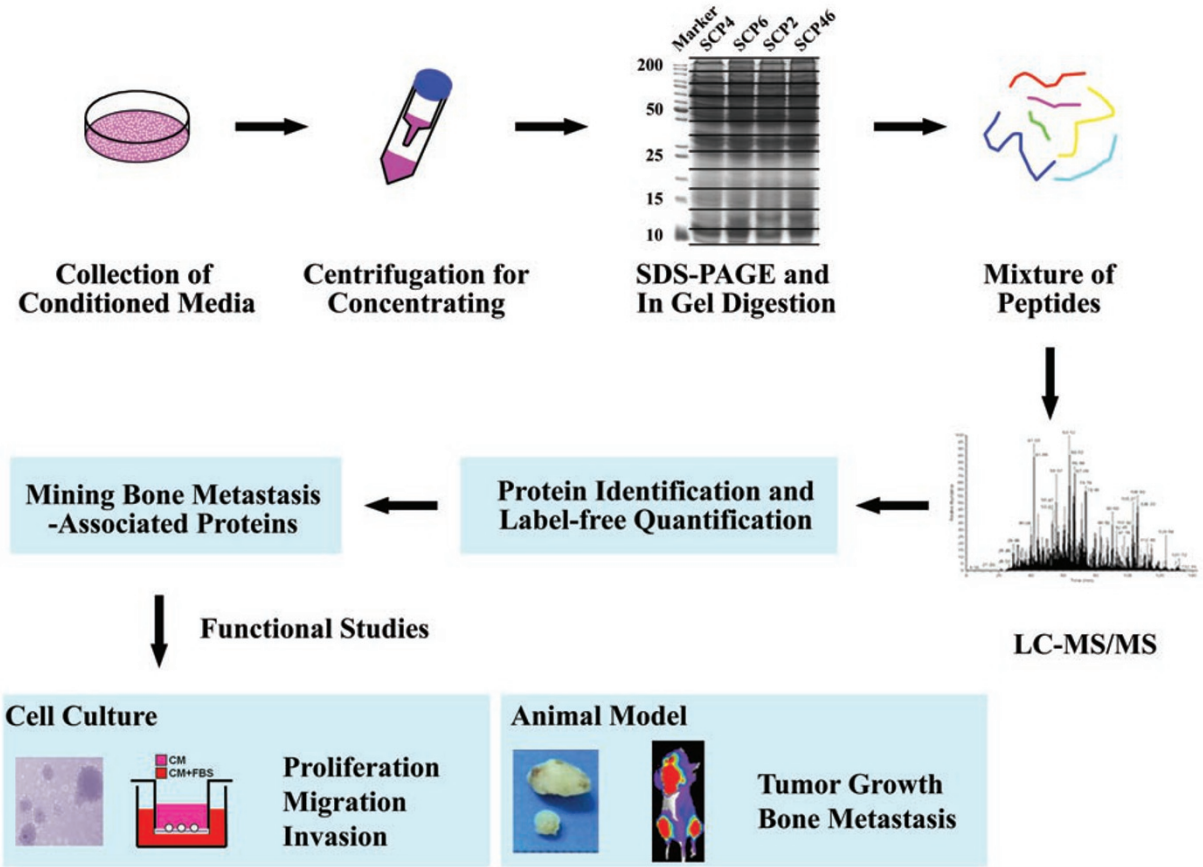

Figure 1 Workflow of the secretome analysis.

Previously Kang *et al*. [29] have analyzed the transcriptomic changes of these same cell lines. Therefore, we analyzed whether the alterations of metastasis-associated secreted proteins can be explained by transcriptional regulation. First, we performed the Gene Set Enrichment Analysis [35] to assess the global gene expression pattern of the 69 up-regulated and 59 down-regulated proteins. As a whole group, the up-regulated proteins were significantly enriched at their mRNA levels in the metastatic cells, and conversely the down-regulated proteins were enriched in the weakly metastatic cells ($P < 10^{-3}$, Figure 3A). Then we analyzed the overlap of bone metastasis-associated proteins with the bone metastasis gene signature previously identified by the transcriptomic analysis [29]. The transcriptomic signature consisted of 106 unique genes, 28 of which encode secreted proteins. Ten (35.7%) of these secreted proteins were found in the list of regulated proteins by the proteomic analysis (Supplementary information, Table S1), an overlap significantly higher than random chances ($P = 6 \times 10^{-10}$). Reciprocally, 33 (25.8%) of the metastasis-associated secreted proteins were regulated transcriptionally with RNA fold changes > 2. However, 78 altered proteins were not regulated obviously in the transcriptional level, and 2 proteins displayed opposite transcriptional alterations, together accounting for 62.5% of the identified proteins (Supple-

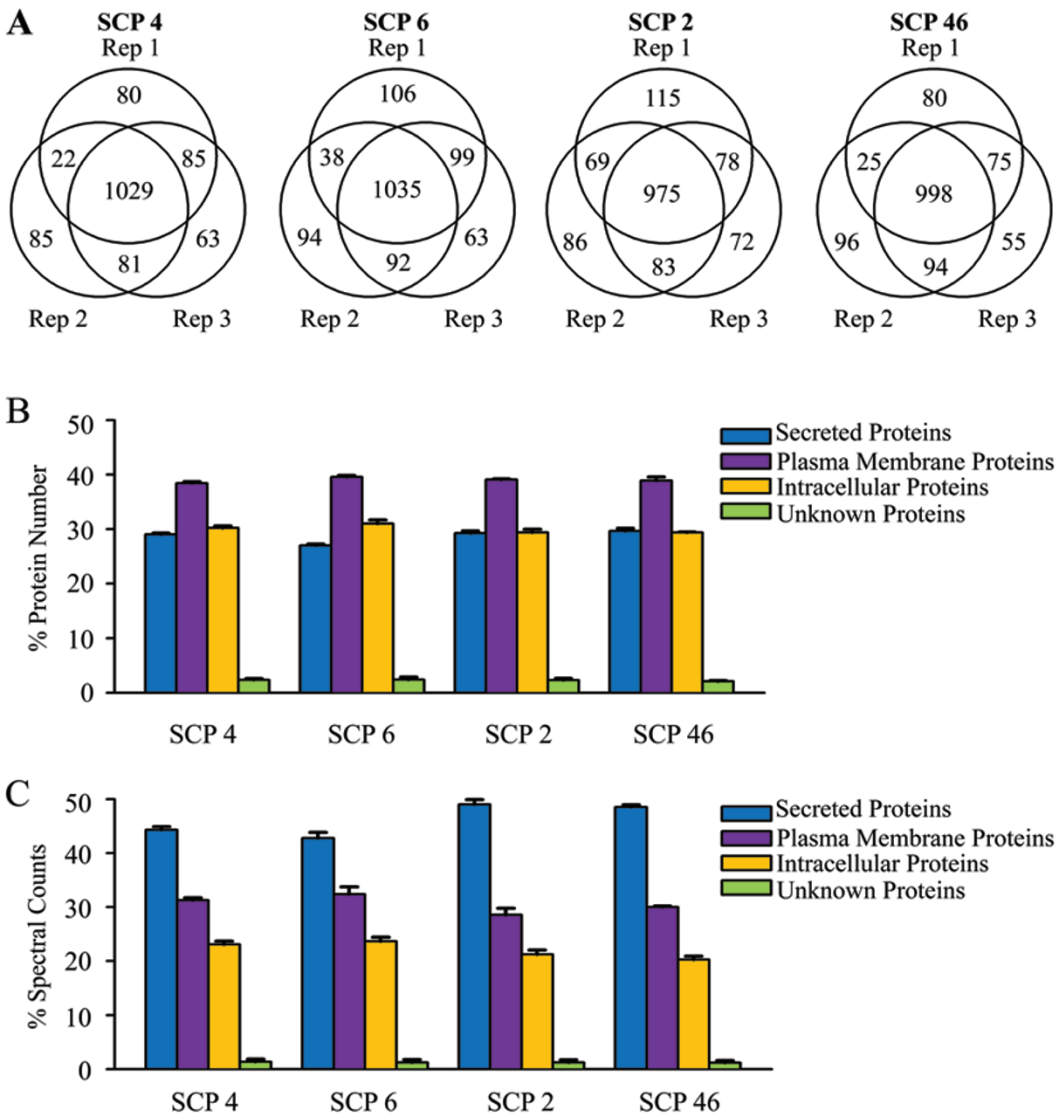

Figure 2 Secretome data overview. **(A)** The overlaps of proteins identified in three independent replicates of each cell line. **(B)** Subcellular localization analyses of the identified proteins. **(C)** Subcellular localization analyses of the identified proteins weighted by their spectral counts.

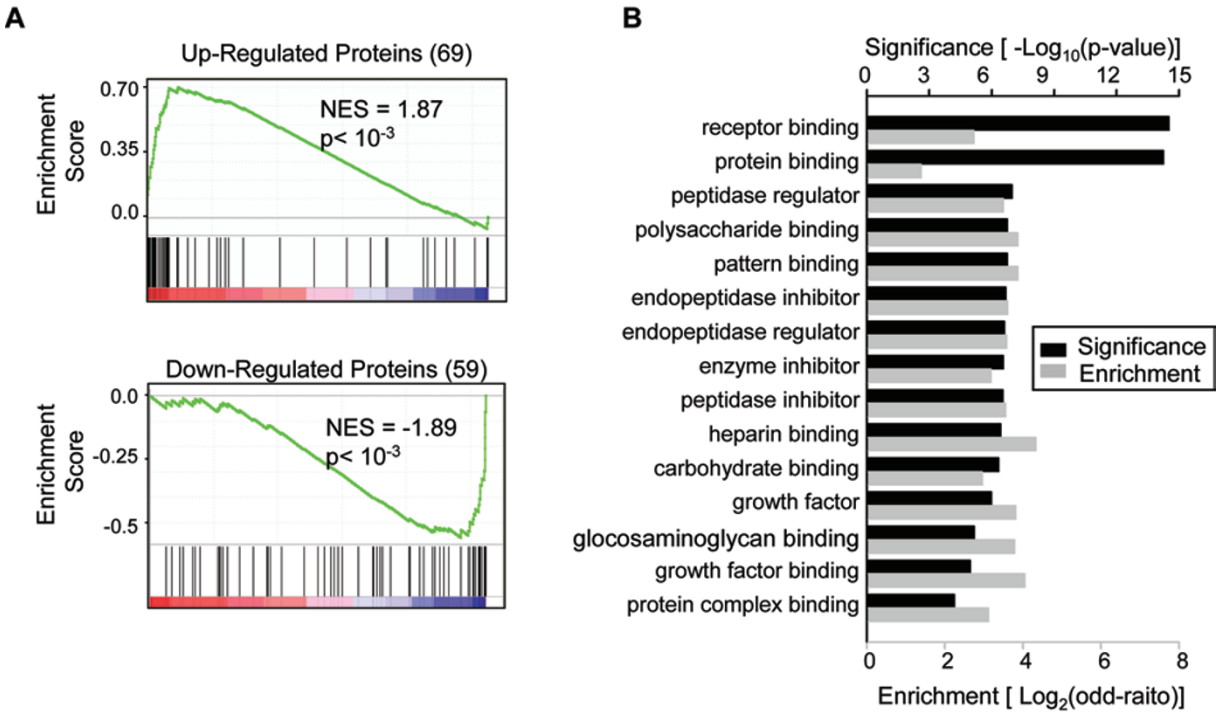

Figure 3 Bone metastasis-associated secreted proteins. **(A)** Gene Set Enrichment analyses of the mRNA expression of up-regulated (top) and down-regulated proteins (bottom) in MDA231 derivatives. The genes were sorted by the mRNA correlation to cancer cell bone metastasis from left (positive correlation) to right (negative correlation). Vertical lines underneath each figure indicate genes matched to the identified secreted proteins. **(B)** Top molecular functions enriched in these proteins.

Table 1 Breast cancer bone metastasis-associated peptidase regulators

Accession no.	Gene symbol	Protein name	SCP 4	SCP 6	SCP 2	SCP 46
IPI00305477	CST1	Cystatin SN	282	436	3343	3032
IPI00013382	CST2	Cystatin SA	23	124	228	211
IPI00032294	CST4	Cystatin S	150	390	2583	2494
IPI00019954	CST6	Cystatin E/M	15	39	0	0
IPI00553177	SERPINA1	Isoform 1 of Alpha-1-antitrypsin	1152	160	35	43
IPI00009890	SERPINE2	Glia-derived nexin	27	68	0	0
IPI00016150	SERPINI1	Neuroserpin	15	16	65	127
IPI00011174	KAL1	Anosmin-1	5	0	50	20
IPI00025418	COL7A1	Isoform 1 of Collagen alpha-1 (VII) chain	36	47	0	5
IPI00218247	TIMP3	Metalloproteinase inhibitor 3	71	192	414	623
IPI00218398	MMP14	Matrix metalloproteinase-14	136	72	231	274
IPI00294004	PROS1	Vitamin K-dependent protein S	36	133	201	212

mentary information, Table S1). The other 15 proteins did not have corresponding microarray probes in the transcriptomic analysis. Therefore, both transcriptional and post-transcriptional regulations were responsible for the alterations of protein secretion during metastasis.

We then performed Gene Ontology (GO) analyses on biological processes and molecular functions of the 128 metastasis-associated proteins. The top enriched biological processes in these proteins were frequently related to cell adhesion and movement (Supplementary information, Figure S2 and Table S3). Molecular function analysis showed that the regulated proteins were

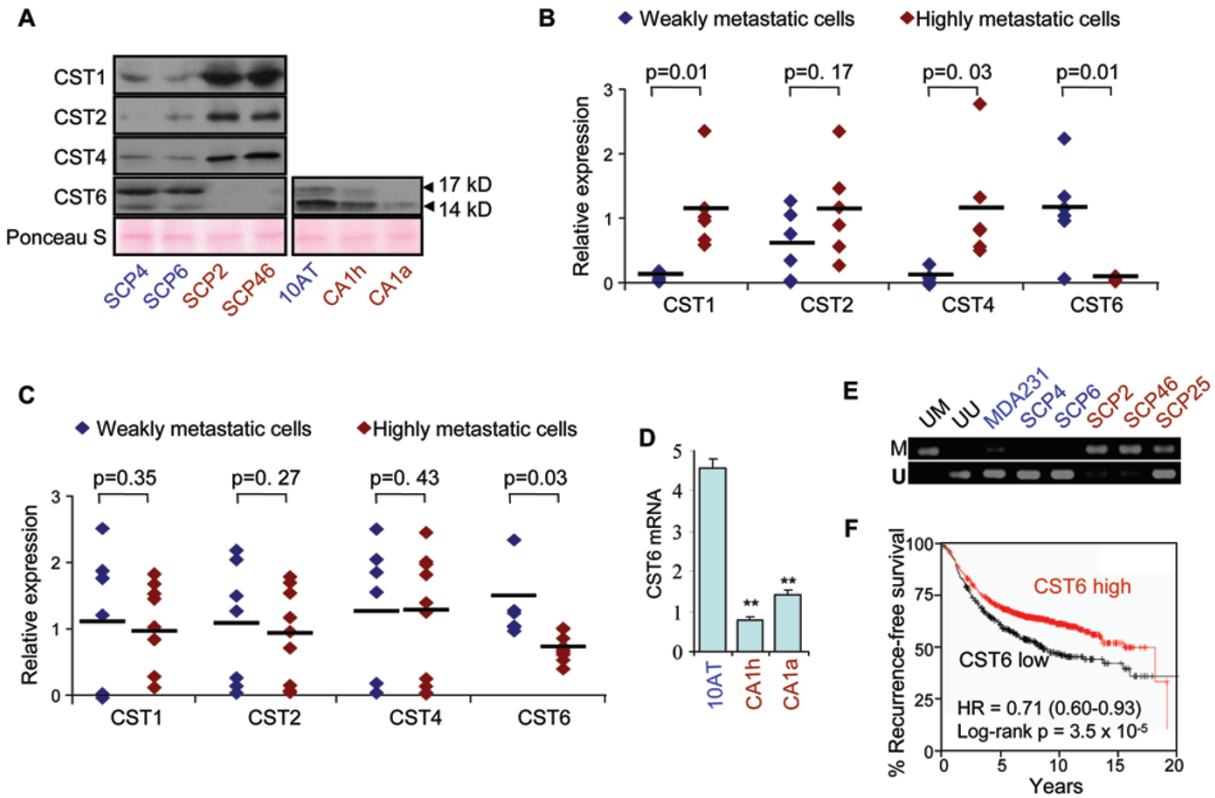

Figure 4 CST6 is negatively correlated with breast cancer bone metastasis. **(A)** Western blot analyses of cystatins in the CM of MDA231 derivatives and MCF10 series. **(B)** Real-time PCR analyses of cystatin mRNA levels in the MDA231 SCP derivatives. Two replicates of each cell line are shown. **(C)** Cystatin mRNA levels in the *in vivo* selected MDA231 derivatives. **(D)** *CST6* mRNA levels in the MCF10 series. **(E)** MSP analysis of the *CST6* promoter. UM, universally methylated DNA; UU, universally unmethylated DNA. **(F)** Kaplan-Meir analysis of breast cancer recurrence in clinical samples.

significantly enriched with those related to protein binding, such as the proteins binding to receptors, polysaccharides and growth factors (Figure 3B and Supplementary information, Table S4), arguing that the extracellular signaling connecting tumor and stromal cells was vital to regulate breast cancer metastasis to bone. Interestingly, other significantly enriched molecular functions of the metastasis-associated proteins were largely involved in regulation of protease activities, especially protease inhibition (Figure 3B). Twelve proteinase regulators, including 4 members of the cystatin family (CST1, CST2, CST4, CST6), 3 members of the serpin family (SERPINA1, SERPINE2, SERPINI1), KAL1, COL7A1, TIMP3, MMP14 and PROS1, were significantly regulated in the secretomes of bone-tropic breast cancer cells (Table 1). All but one (MMP14) of these regulators were inhibitors of proteinases, such as cysteine proteinases, serpin peptidases and metalloproteinases, suggesting the roles of these proteinases in shaping the tumor microenvironment during the spreading of cancer cell to bone.

CST6 expression and secretion are negatively correlated with bone metastasis

In the list of bone metastasis-associated secreted proteins, the most well-represented proteinase inhibitor family was cystatins, the type 2 members of the cystatin superfamily [36]. Cystatins are endogenous inhibitors of lysosomal cysteine proteinases including cathepsins, papain and legumain. These proteinases and cystatins counteracted each other to tailor the proteolytic activities inside and outside the cells, which is critical for cell signaling, apoptosis, ECM modeling and tumorigenesis [36]. Our proteomics data indicated that these proteins might also play important roles in breast cancer bone metastasis. Four cystatins, namely CST1, CST2, CST4 and CST6, were aberrantly regulated in the CM of bone-tropic cells. CST6 secretion in bone-metastatic cells was suppressed, while secretions of the other three cystatins were elevated. Therefore, we focused on these cystatins for further screening. We first validated the secretion levels of cystatins in the CM of cancer cells by western

blot analysis. Consistent with the proteomic analysis, CST1, CST2, CST4 were abundantly present in the CM of bone-metastatic cells SCP2 and SCP46, while they were significantly less secreted by the weakly metastatic cells SCP4 and SCP6. In contrast, both forms of the CST6 protein, the 14 kD form and the glycosylated 17 kD form, were readily observed in the CM of SCP4 and SCP6, whereas neither form could be detected in the CM of SCP2 or SCP46 (Figure 4A).

Next we tested the cystatin mRNA expression in a wider array of breast cancer cell lines with different metastasis potentials. In the MDA231 SCP derivatives, the expression patterns of cystatins were generally consistent with their secretion levels. *CST1* and *CST4* were expressed more abundantly in SCP2, SCP46, and another two bone-tropic lines SCP20 and SCP25, than in SCP4, SCP6 and another mildly metastatic line SCP28. *CST2* displayed a similar expression pattern, albeit without statistical significance. In contrast, *CST6* was expressed only in the weakly or mildly metastatic cells, but not in the highly metastatic cells (Figure 4B). We further analyzed transcriptomic microarray data for a separate group of 18 *in vivo* selected MDA231 derivative cell lines, including the weakly metastatic lines 1834, 2293, 2295, 2297, 4142, 4180 and the bone-tropic lines 1833, 2268, 2269, 2271, 2274, 2287, PD1, PD2A, PD2B, PD2C, PD2D, PD2E. These cell lines were either obtained by *in vivo* selection of rare cell variants pre-existing in the MDA231 population [29], and Kang *et al.*, personal communication), or resulted from *in vivo* evolution of non-metastatic cells after a long-term dormancy [37]. In this cell group representing two model systems for breast cancer bone metastasis that are distinct from the SCP derivatives, the expression of *CST6* by the bone-tropic cells was consistently weaker than that by the non-metastatic cells. However, the mRNA expression levels of other cystatins were not correlated with cancer cell bone-tropism (Figure 4C). We also examined the expression of cystatins in the MCF10 cell line series including MCF10AT, MCF10CA1h and MCF10CA1a. These isogenic human breast cancer cell lines display progressively increased metastatic malignancy when injected into immunodeficient mice. The *CST6* expression level was much higher in the less malignant MCF10AT than in the other two lines (Figure 4D), but other cystatins did not show any difference in their expression (data not shown). In addition, the CST6 extracellular protein level declined gradually in the MCF10 series, but with a lesser extent of glycosylation than in the MDA231 derivatives (Figure 4A). Therefore, the *CST6* expression was consistently correlated with metastasis in different cell models.

It has been reported that the *CST6* gene was often silenced by DNA methylation in breast cancer cells [38, 39]. Thus we studied the methylation levels of a CpG island on the *CST6* promoter in MDA231 derivative cells by methylation-specific PCR (MSP) and bisulfite sequencing. Both assays showed that the *CST6* promoter was specifically methylated in the metastatic cells (Figure 4E and Supplementary information, Figure S3). The first 3 CpG loci were heavily methylated in SCP2, SCP46 and SCP25 in which *CST6* was not expressed, while methylation of these loci was rarely observed in the *CST6*-expressing SCP4, SCP6 and MDA231 parental cells (Supplementary information, Figure S3).

We then analyzed the clinical significance of *CST6* expression in human breast tumors with Kaplan-Meier Plotter, an online tool to evaluate the correlation of gene expression with breast cancer prognosis in over 2300 clinical samples [40]. With this tool, we found that lower expression of *CST6* was linked to markedly higher risk of breast cancer recurrence (hazard ratio = 0.71, $P = 3.5 \times 10^{-5}$), establishing CST6 as a prognosis marker for breast cancer (Figure 4F). We further compared the CST6 expression in breast cancer primary tumors and bone metastases from a clinical microarray dataset [41] and found that CST6 was down-regulated in the bone metastasis tissues (Supplementary information, Figure S4). Therefore, we focused on CST6 for functional validation in the further studies.

CST6 inhibits in vitro migration and invasion of breast cancer cells

CST6 has been previously noticed to be down-regulated in malignant breast tumor cells [42, 43]. However, its functional role in metastasis, especially in bone metastasis, has yet to be fully characterized. We first stably overexpressed *CST6* in the highly metastatic SCP2 cells with a retroviral plasmid. Real-time PCR and western blot analyses confirmed that *CST6* was overexpressed, which led to the elevated secretion of the protein (Figure 5A). We also confirmed that the ectopic CST6 protein was biologically functional in that it inhibited the enzymatic activities of cathepsin B (CTSB) and L (CTSL), two of its target proteinases (Figure 5B). *CST6* overexpression suppressed cancer cell growth and soft-agar colony formation (Figure 5C and 5D), suggesting a role of CST6 in breast cancer tumorigenicity. We then tested the effect of *CST6* overexpression on cell migration via the wound-healing assay and observed nearly 50% impairment of cell motility by CST6 (Figure 5E). By two-chamber transwell assays, we also found that CST6 diminished SCP2 migration by 8-fold (Figure 5F) and invasiveness by 3-fold (Figure 5G). The suppressive role of CST6 in cancer cell invasion was also observed when

we overexpressed *CST6* in another breast cancer cell line MCF10CA1h. *CST6* overexpression in MCF10CA1h resulted in elevated CST6 secretion and significantly reduced cell invasion (Figure 5H).

To determine whether CST6 inhibition was sufficient to promote cancer cell malignancy, we used two independent short hairpin RNA (shRNA) constructs to knock down *CST6* in SCP4 cells. Both constructs efficiently silenced *CST6* in SCP4 and abrogated the secreted protein in CM (Figure 6A). Concordant to the observations after *CST6* overexpression, *CST6* knockdown in SCP4 promoted cancer cell proliferation, soft-agar colony formation, wound-healing motility, transwell migration and invasion (Figure 6B-6G). We also knocked down *CST6* in MCF10AT that expressed *CST6* abundantly and found a similar phenotype (Figure 6H), suggesting that breast cancer cells indeed acquire malignant traits by silencing *CST6*.

Although the overexpression and knockdown experiments proved that CST6 functioned to repress cancer cell malignant progression, it was still unclear whether CST6 exerted its roles inside the cells or extracellularly. Thus we tested the CST6 protein function in the cancer cell culture medium. The CM of SCP2 overexpression cells contained a higher concentration of CST6 than that of the control cells (Figure 5A). Thus we tested the transwell migration capability of untransfected SCP2 in the CM of SCP2 control and overexpression cells. The CM containing abundant CST6 protein significantly attenuated the

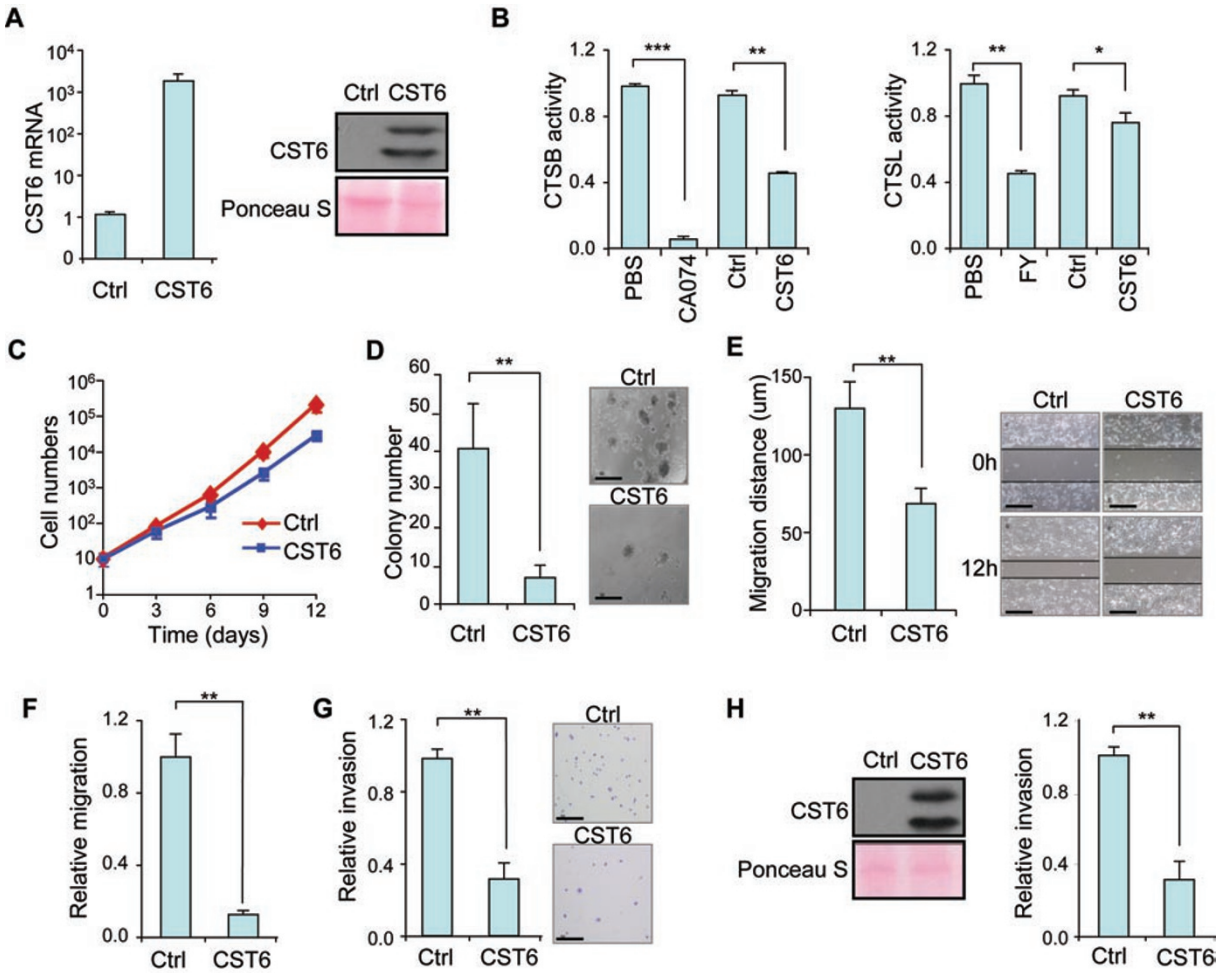

Figure 5 *In vitro* functional analyses of *CST6* overexpression. **(A)** *CST6* mRNA levels and CM protein levels in SCP2 control and overexpression cells. **(B)** Overexpressed CST6 inhibited the enzymatic activities of CTSB and CTSL. The cathepsin inhibitors epoxysuccinyl peptide (CA074) and Z-FY(t-Bu)-DMK (FY) were used as controls. **(C-G)** *In vitro* growth rates **(C)**, soft-agar colony formation **(D)**, wound-healing **(E)**, transwell migration **(F)** and invasion **(G)** of SCP2 control and overexpression cells. **(H)** *CST6* overexpression in MCF10CA1h and the transwell invasion analysis. Student's *t*-test $*P < 0.05$; $**P < 0.01$. Scale bar, 200 μm.

migration of SCP2 cells (Figure 7A). Conversely, when we knocked known *CST6* in SCP4 to abolish the CST6 protein in the CM, the SCP4 CM could result in substantially elevated migration of SCP2 cells (Figure 7A). We performed these experiments again for SCP4 cells cultured in the same collection of CM. Consistently, cancer cells seeded in CM without the CST6 protein displayed much higher migratory capabilities (Figure 7B). In addition, when SCP2 or SCP4 cells were cultured in the CM of SCP4, they migrated slower than the same cells cultured in the CM of SCP2 that contained less soluble CST6 (Figures 4A, 7A and 7B). Further, we used a neutralizing anti-CST6 antibody to block the CST6 protein in the CM of *CST6*-overexperssion cells, and found that the migration-inhibitory effect of the CM could be reversed completely by the antibody in a dose-dependent manner (Figure 7C). The neutralizing antibody was also able to abolish the migration-inhibitory effect of the CM from SCP4 cells (Figure 7D). However, when the soluble CST6 was ablated from the SCP4 CM by shRNA knockdown, the neutralizing antibody had no effects on cell migration (Figure 7D). Taken together, these data showed that secreted CST6 suppressed cancer cell migration.

In addition to cancer cells, stromal cells could also contribute to the secreted factors in the tumor microenvironment. We then analyzed whether other cell components of breast tumor tissues secret CST6 by western blot and immunohistochemistry analyses. It was shown that only normal mammary epithelial cells and tumor cells expressed CST6, while cell lines of the M2 macrophage, endothelium, fibroblast or stromal cells surrounding breast tumors did not secret visible levels of CST6 (Supplementary information, Figure S6), which is consistent to previous findings regarding the tissue specificity of CST6 expression [44, 45].

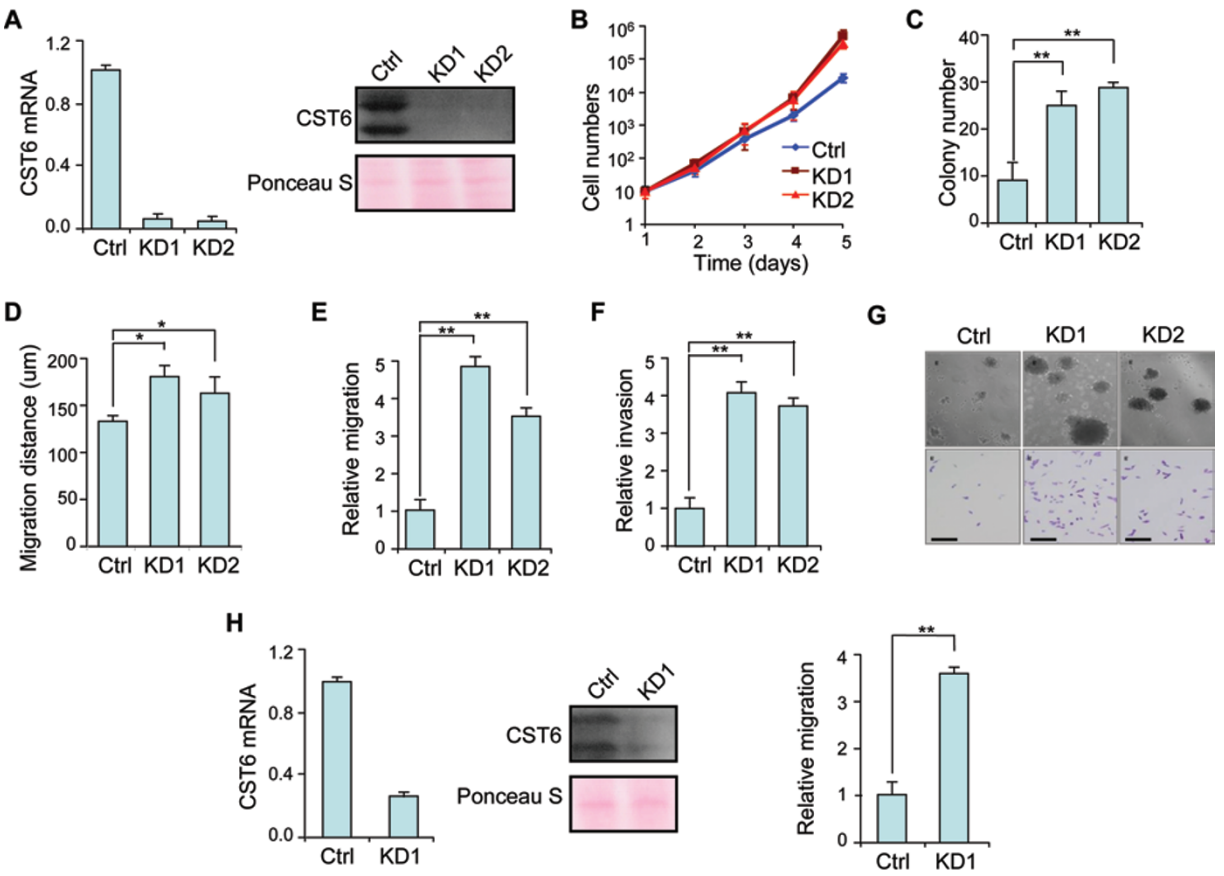

Figure 6 *In vitro* functional analyses of *CST6* knockdown. **(A)** *CST6* mRNA and CM protein levels in SCP4 control and knockdown cells. **(B-F)** *In vitro* growth rates **(B)**, soft-agar colony formation **(C)**, wound-healing **(D)**, transwell migration **(E)** and invasion **(F)** of SCP4 control and knockdown cells. **(G)** Representative images of colony formation (top) and transwell invasion assays (bottom). **(H)** *CST6* knockdown in MCF10AT and the transwell migration analysis. Student's *t*-test $*P < 0.05$; $**P < 0.01$. Scale bar, 200 μm.

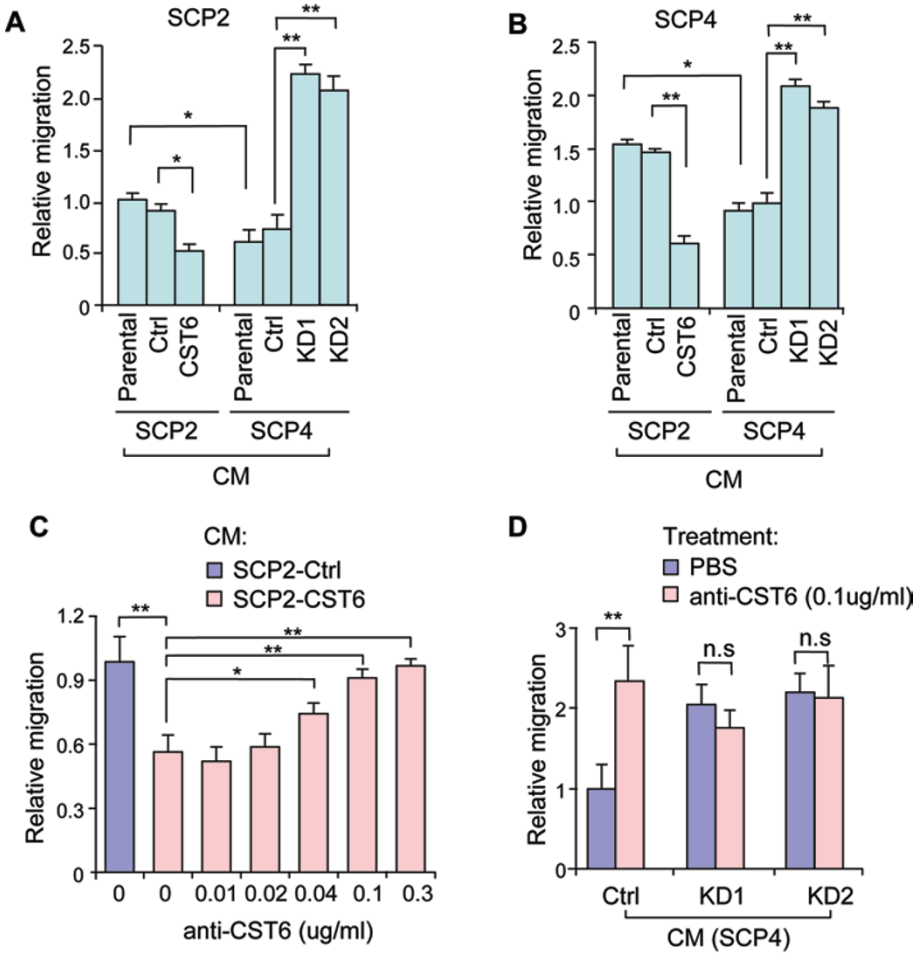

Figure 7 Secreted CST6 suppresses cell migration. **(A)** Trans-well migration analyses of SCP2 cells cultured in the serum-free CM from SCP2 parental, control and overexpression cells, or CM from SCP4 parental, control and knockdown cells. **(B)** Trans-well migration analyses of SCP4 cells cultured in the same set of CM. **(C)** The effects of SCP2 CM with various concentrations of neutralizing CST6 antibody on SCP2 cell migration. **(D)** The effects of SCP4 CM with or without neutralizing CST6 antibody on SCP2 cell migration. Student's *t*-test **P* < 0.05; ***P* < 0.01; n.s, not significant.

CST6 suppresses breast cancer bone metastasis

We further tested the *in vivo* function of CST6 in breast cancer using a xenograft mouse model. We first injected the SCP2 cells with or without *CST6* overexpression into the mammary fat pads of nude mice, and found that primary tumor growth was greatly impaired by CST6 (Figure 8A). We then examined the effect of CST6 on metastatic tumor growth at distant organs. The SCP2 cells were labeled with a plasmid construct expressing firefly luciferase and injected into the left ventricle of nude mice for bone metastasis analyses. The bone metastasis burden of mice was quantitated weekly by non-invasive bioluminescent imaging (BLI). *CST6* expression in the cancer cells markedly reduced metastasis signals in the spine and limbs (Figure 8B, 8C and Supplementary information, Figure S7). By the 10th week after cancer cell injection, the metastasis burden caused by *CST6*-expresssing cells was nearly 10 times weaker in the spine and 20 times weaker in hindlimbs than that by control cells. The control SCP2 cells resulted in severe osteolytic bone lesions and massive bone destruction in the femurs at that time. In contrast, the cells expressing *CST6* led to much milder bone damages and tumor lesions (Figure 8B and 8C). In addition, when we extracted the bone marrow from the femur and tibia at the 10th week and seeded the marrow in culture medium supplemented with puromycin that would eliminate all host cells, much fewer cancer cell colonies grew from the marrow of mice injected with *CST6*-expressing cancer cells (Figure 8B). Moreover, *CST6* overexpression significantly prolonged mouse survival after cancer cell implantation. Eight of 9 (89.9%) mice bearing the control SCP2 cells died

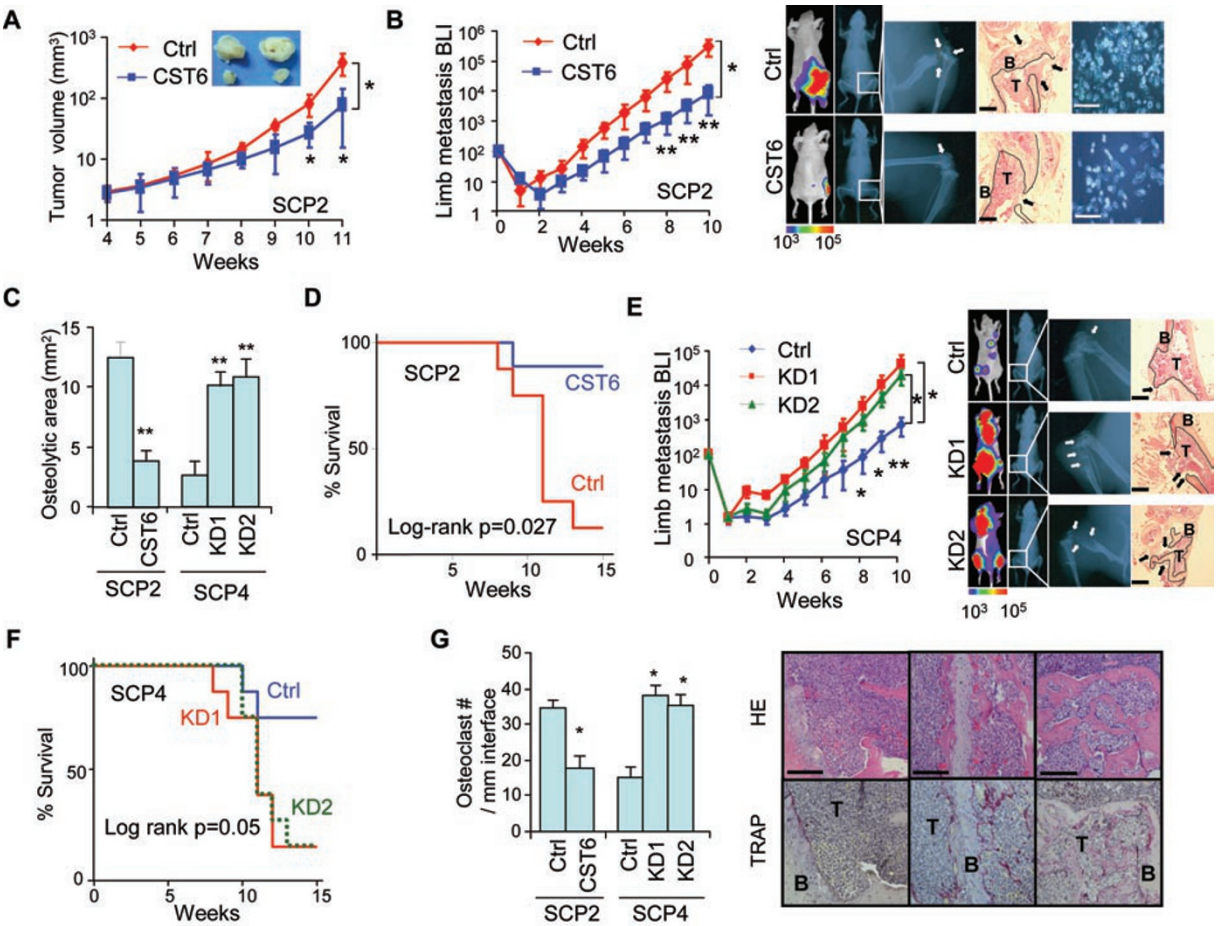

Figure 8 CST6 suppresses *in vivo* bone metastasis. **(A)** Primary tumor growth from SCP2 control and overexpression cells. Scale bar, 4 mm. **(B)** The hindlimb metastasis burden of nude mice after intracardiac implantation of SCP2 cells. Shown at the right are BLI, X-ray, histological images and cancer cell colonies seeded from the bone marrow of mouse femurs. **(C)** Quantification of osteolytic areas in the hindlimbs from X-ray analysis. **(D)** Survival analysis of mice injected with SCP2 control and overexpression cells. **(E)** Metastasis burden in the hindlimbs after intracardiac implantation of SCP4 control and knockdown cells, and the BLI, X-ray and histological images. **(F)** Survival analysis of mice injected with SCP4 control and knockdown cells. **(G)** TRAP staining analysis of bone lesions (right) and the quantitation of osteoclast numbers along the tumor-bone interface (left). *Student's *t*-test (individual time points) or repeated measures ANOVA (growth curves) $P < 0.05$; **$P < 0.01$. Arrows in **B** and **E** indicate areas of overt bone destruction. Dotted lines denote interface of bone and tumor lesions. B, bone; T, tumor. Scale bar, 1 mm (histology in **B** and **E**) or 200 μm (others).

from severe metastasis burden 15 weeks post injection, while only 1 of 8 (12.5%) mice succumbed to the *CST6*-expressing cells at the same duration (Figure 8D).

We then tested the metastasis effect of *CST6* knockdown in the SCP4 cells. Both *CST6* shRNA constructs in the cancer cells resulted in more aggressive metastasis in the spine and limbs of nude mice (Figure 8E and Supplementary information, Figure S7). At the 10th week after injection, the control SCP4 cells only led to minor bone damages in the limbs. The tumor lesions remained mostly within the bones. In contrast, the mice injected with *CST6*-knockdown cells suffered from widely-spread metastatic tumors and immense bone loss in the femurs and tibia. *CST6* knockdown also accelerated animal deaths (Figure 8F).

To further analyze the effect of CST6 on osteolysis during bone metastasis, we performed TRAP staining on the metastasis tumors to assess the mature osteoclasts along the interface of tumor cells and bone matrix. We found that *CST6*-expressing cancer cells were surrounded by markedly less osteoclasts as compared to the control cells, while *CST6* knockdown led to increased numbers of osteoclasts (Figure 8G). Collectively, the animal studies demonstrated that CST6 significantly suppressed os-

teolytic bone metastasis of breast cancer cells.

Discussion

In this study we systemically analyzed the tumor secreted proteins that were associated with breast cancer bone metastasis. To our knowledge, this is the first fully published secretome study for bone metastasis of breast cancer. The skeleton is the major target site of metastasis for many types of cancer including breast cancer [2]. Elucidating the secretomic anomaly of tumor cells during skeleton metastasis may help decipher the molecular events that enhance the compatibility of metastasizing cancer cells and bone stroma. More importantly, given the nature of secreted proteins to be readily detected and readily targetable by therapeutics, the identification of bone metastasis-specific secreted proteins will provide us a good source of candidate molecules for prognosis prediction and anti-cancer intervention.

Previous transcriptomic studies of breast cancer metastasis organotropism have led to the identification of a number of molecules that are correlated with metastasis to various organs such as the lungs, bone and brain [29, 46, 47]. Comparison of the bone metastasis protein signature with the transcriptomic signature identified by gene expression profiling revealed 10 proteins that were regulated concordantly in the transcriptional level and the secretion level. Many of them, such as ADAMTS1, CTGF, IL11 and MMP1, are well-proven functional mediators of metastasis [29, 48]. However, transcriptional regulation could only explain approximately one quarter of the secretomic difference. The transcriptional alterations of 74.2% of bone metastasis-specific secreted proteins were either unknown, not obvious, or even opposite to the proteomic analysis results, indicating an important role of post-transcriptional regulation for metastasis-related secretion. Some of these molecules, such as JAG1 and IGFBP3 [31, 49], have been already demonstrated to impact the metastasis of breast cancer cells. Therefore, the discovery of metastasis-specific regulation at the protein level will not only bring in novel candidates of metastasis functional molecules, but also improve our understanding of the metastasis process from a different angle.

In addition to the aforementioned proteins that are proven functional molecules in bone metastasis, some proteins in the regulated list, such as BMP1, BMP4, TIMP3, ITGA3 and ICAM2, are promising candidates for further studies. BMP1 and BMP4 are potent regulators of bone formation and have been implicated in skeleton metastasis [50]. TIMP3 regulates bone formation and excessive TIMP3 in bone may induce osteoblast differentiation, leading to depletion of osteoblast progenitors in the bone marrow [51]. ITGA3 is the receptor for collagen and thus can mediate the interaction of cancer cells to ECM. ICAM2 regulates the cell cytoskeleton reorganization and suppresses neuroblastoma metastasis [52]. Therefore, these proteins are likely to promote or suppress bone colonization of breast cancer cells. Validation of their roles in metastasis and elucidation of the functional mechanisms will greatly help to understand the biology underlying bone complication of breast cancer.

Cysteine proteinases, serpin peptidases and metalloproteinases are known to play critical roles in tumor initiation, progression and metastasis [9, 53-55]. The search for chemical compounds to inhibit these proteinases is a topic of constant interest for anti-cancer therapeutics [56, 57]. Notably, the bone metastasis-specific proteins identified in our proteomic study are enriched with the regulators of these proteinases. This data indicated that not only the proteinases but also their endogenous regulators were subject to tight regulation during metastasis, suggesting a new direction for drug designing to target proteinases in therapeutics.

CST6 is the natural inhibitor of lysosomal proteases CTSB, CTSL, cathepsin V (CTSV) and legumain (LGMN). Its physiological expression is restricted to mammary epithelium, the stratum granulosum of skin epidermis, sweat glands, hair follicle and nail [44, 45]. The balance of CST6 and its target proteinases is essential for the homeostasis of these tissues [44, 58]. CST6 knockout in mice causes neonatal lethality due to excessive transepidermal water loss [59]. In this work, we selected CST6 for functional validation in breast cancer bone metastasis, due to the fact that the cystatin family proteins were collectively regulated in bone metastasis and, in particular, CST6 was consistently correlated with breast cancer metastasis in a wide range of cell lines and clinical samples. Disregulation of cystatins in cancer cells has been widely reported [36]. Among them, CST6 is generally regarded as a tumor suppressor as it is often silenced in tumor cells, especially in metastatic cells [42, 60-63]. However, the observations in CST6 functional analyses have been conflicting. While some studies reported the suppressive roles of CST6 in tumor cell proliferation, migration and invasion of several cancer types [42, 64, 65], it was also found to promote pancreatic cancer growth [66]. In breast cancer, *CST6* was originally identified as a gene down-regulated in a metastatic cell line as compared to its matched primary tumor cell line [67-71]. Since then, data have been accumulated to show its silencing, mostly by epigenetic regulation, in breast cancer [72], whereas few studies

reported the functional characterization of CST6. The functions of CST6 in breast cancer have been tested mainly in the MDA-MB-435 cell line, demonstrating that *CST6* overexpression delayed the metastasis growth in lungs and liver but had no effect on the metastasis incidence in these organs [73]. However, the lineage fidelity of MDA-MB-435 to breast epithelium is currently in debate [74]. In addition, the function analysis was performed exclusively by forced expression of *CST6*, and it has been unclear whether cancer cells can acquire malignant traits by *CST6* loss. Therefore, solid evidence is yet needed to support the function of CST6 in breast cancer metastasis, especially to bone. Furthermore, it is unknown how CST6 plays its roles in metastasis.

We performed rigorous functional analyses and found that CST6 suppressed cancer cell proliferation, colony-formation, migration and invasion. The phenotypes were observed with both approaches of overexpression and knockdown. Ectopic expression of *CST6* weakened the aggressiveness of cancer cells, while two independent knockdown constructs of *CST6* resulted in increased malignancy. More importantly, the CST6 displayed an obviously suppressive role to breast cancer bone metastasis in the animal studies. While control SCP2 cells formed metastasis rapidly in spine and limbs of nude mice and caused massive osteolysis, the same cells with *CST6* overexpression showed significantly weaker virulence in the animals. In addition, the mice were rescued from metastasis-caused deaths by *CST6* overexpression. Moreover, *CST6* inhibition by shRNA in a less virulent cell line SCP4 caused the opposite changes, documenting the evidence that loss of CST6, a phenomenon often observed in aggressive breast carcinoma, confers the cells more malignant traits including bone-tropism. Therefore, our study firmly established CST6 as a suppressor of breast cancer bone metastasis.

In addition, we showed that CST6 exerted its function in the extracellular space. The CM containing high or low levels of soluble CST6 protein caused the cancer cells to migrate differently, and blocking the secreted CST6 by a neutralizing antibody abolished such difference. We could not rule out the possibility that intracellular CST6 plays a role in metastasis as well. Nevertheless, secreted CST6 was shown to suppress breast cancer bone metastasis. This is important for CST6 to be considered as a prognosis marker or a druggable molecule, as it is much easier to detect CST6 in the serum or body fluid than in tumor cells, as well as to deliver the recombinant CST6 or the inhibitors of its downstream proteinases to the extracellular space.

Intriguingly, 3 other family members of cystatins, CST1, CST2 and CST4, displayed a disregulation pattern totally opposite to that of CST6 in metastasis. Although CST1/2/4 were also lysosomal protease inhibitors as CST6, they may have different target specificities. Previous studies reported that CST6 inhibits CTSB, CTSL, CTSV and LGMN, while the other cystatins primarily target on papain, ficain, with CST1 inhibiting CTSB as well [75]. Indeed, our analysis demonstrated that SCP2 and SCP4 cells expressed and secreted these proteinases at various levels. CST6 inhibited CTSB and LGMN efficiently, but CST1 only suppressed the enzymatic activity of CTSB and the other two cystatins had no effects on either proteinases (Supplementary information, Figure S5). Therefore, the difference in target preference might provide an explanation of the marked discrepancy in the secretion of cystatin proteins, which, however, is to be further studied.

In conclusion, this study identified the secreted proteins that were regulated during breast cancer bone metastasis in an isogenic cell line model. Caution needs to be taken to interpret these results as cell line models may not well represent the clinical metastatic disease. Nevertheless, these candidate proteins hold great promise to further investigate the molecular underpinning of breast cancer bone tropism. In addition, this study revealed CST6 as a metastasis suppressor that is silenced in breast tumor cells metastatic to bone. Therefore, it potentially can serve as a prognosis biomarker, and can be applied in cancer therapeutics with approaches such as gene therapy or recombinant protein delivery. Future work is needed to define its downstream effectors so that alternative therapeutic methods can be used to block the metastasis pathways that are naturally inhibited by CST6.

Materials and Methods

Cell culture

MDA231 parental and derivative cells were cultured in Dulbecco's Modified Eagle's Medium (DMEM, HyClone) supplemented with 10% fetal bovine serum (FBS, HyClone), 100 units/ml penicillin and 100 μg/ml streptomycin (Invitrogen) in 5% CO_2 at 37 °C. MCF10 cell line series were maintained in DMEM/F12 medium supplemented with 5% horse serum, 10 μg/ml insulin (Roche), 20 ng/ml epidermal growth factor (Invitrogen), 100 ng/ml cholera toxin (Merck), 0.5 μg/ml hydrocortisone (Enzo), penicillin and streptomycin. For bioluminescent imaging, cell lines were retrovirally infected with a fusion protein construct encoding the green fluorescent protein and the firefly luciferase.

Plasmids and antibodies

Human CST6 was cloned into the pMSCVpuro plasmid (Clontech) for overexpression. *CST1*, *CST2*, and *CST4* overexpression plasmids were kind gifts from Dr Yibin Kang at Princeton University. The shRNA target sequences for *CST6* knockdown

were 5′-GCCGTATCTGTCACAATAA-3′ (KD1) and 5′-GTGGTTCCCTGGCAGAACT-3′ (KD2). The shRNA sequences were cloned into the pSuper-Retro-Puro retrovirus vector (OligoEngine). The goat anti-human CST6 (R&D Systems) was used in this study for western blot, immunohistochemistry and neutralizing analyses. The rabbit anti-human CST1 (Proteintech), rabbit anti-human CST2 (Proteintech), rabbit anti-human CST4 (Abgent), mouse anti-human CTSL (R&D), goat anti-human CTSB (R&D) and goat anti-human LGMN (R&D) were used for western blot.

CM collection

Cells were grown to ~80% confluence in 10 cm culture dishes. After washing with serum-free medium at 37 °C for 15 min twice and 60 min twice, the cells were incubated in serum-free medium at 37 °C for 24 h. The cell death rate was controlled at below 3% (measured by trypan blue staining). The CM were collected, centrifuged at 1 000 rpm for 10 min, filtrated by 0.22 μm filters, and then added with protease inhibitors (Roche). The collected CM were stored at −80 °C until used.

One-dimensional gel electrophoresis and in-gel digestion

The CM were concentrated with the Ultra-15 centrifugal filter devices with the 3-kD cutoff (Millipore), and the protein concentration was determined by Bradford assay. Concentrated CM containing 35 μg proteins of each sample were subjected to SDS-PAGE and stained with Coomassie blue. After extensive decolorization, each lane was excised into 12 sections. Each section was cut into ~1 mm cubes and destained by incubation using 50% acetonitrile in 50 mM ammonium bicarbonate. After destained, the gel pieces were reduced by incubation in a solution of 50 mM Tris (2-carboxyethyl) phosphine in 25 mM ammonium bicarbonate at 60 °C for 10 min. For alkylation of proteins, the gel was incubated in 100 mM iodoacetamide (IAA) at room temperature for 60 min, followed by washing with 50% acetonitrile in 50 mM ammonium bicarbonate twice. The gel pieces were then dehydrated in 100% acetonitrile for 15 min, dried completely by SpeedVac, swollen in 50 μl of 25 mM ammonium bicarbonate containing 0.01 μg/μl trypsin (Promega) and incubated overnight at 37 °C. Peptides were extracted with 50% acetonitrile containing 5% formic acid four times, dried by vacuum centrifugation at 60 °C, and stored at −20 °C for further analysis.

Nano LC-MS/MS

All nano LC-MS/MS experiments were performed on the MDLC system (Michrom Bioresources Inc.) coupled with a Thermo Finnigan 2-D linear ion trap mass spectrometer (LTQXL, Thermo Inc.). The trypsin-digested dry sample was dissolved in 30 μl 5% acetonitrile with 0.1% formic acid, and 20 μl of this peptide solution was loaded onto a Peptide Captrap column (Michrom Bioresources Inc.) with the autosampler of the MDLC system. To desalt and concentrate the sample, the trap column was washed with 5% acetonitrile containing 0.1% formic acid at a flow rate of 10 μl/min for 10 min. Then the trapped peptides were released and separated on a C18 capillary column (0.1 mm i.d. × 150 mm, 3 μm, 200 Å, Michrom Bioresources Inc.). The flow rate was maintained at 500 nL/min. Mobile phase A was 0.1% formic acid in water, and mobile phase B was 0.1% formic acid in acetonitrile. The eluted gradient was started at 5% B, reached 35% B in 120 min, then 80% B in the next 2 min. The LC setup was coupled online to a LTQ using a nano-ESI source (ADVANCE, Michrom Bioresources Inc.) in the data-dependent acquisition mode (m/z 400-1800). The temperature of heated capillary was set at 200 °C and spray voltage was 1.2 kV. The mass spectrometer was set as one full MS scan followed by ten MS/MS scans on the ten most intense ions from the MS spectrum with the following dynamic exclusion settings: repeat count = 2, repeat duration = 15 s, exclusion duration = 30 s.

Protein identification

All data files were created by searching MS/MS spectra against the Human International Protein Index protein sequence database (IPI.Human.v3.67.fasta, 84118 entries), using the TurboSEQUEST program in the BioWorks 3.3 software suite, with a precursor-ion mass tolerance of 2.0 amu and fragment-ions mass tolerance of 0.8 amu. Trypsin was set as the protease with two missed cleavage sites allowed. Carbamidomethylation (+57.02150 Da) was searched as a fixed modification on cysteine, representing alkylation with IAA, while oxidized methionine (+15.99492 Da) was searched as variable modifications. The searched peptides and proteins were validated by PeptideProphet1 and ProteinProphet2 in the Trans-Proteomic Pipeline (TPP, v. 4.2) using default parameters. Proteins with ProteinProphet *P*-value greater than 0.9 and no less than three kinds of unique peptides were considered as true identifications. Randomized IPI.HUMAN.v3.67.fasta was used as a decoy database to estimate the false discovery rate (FDR) of protein identification. The FDR was calculated as the ratio of the number of matches on the randomized database to the sum of randomized matches and observed matches. FDR for ProteinProphet 0.9 in our analysis was < 1%. Proteins containing the same peptides were grouped, and only one protein with the highest probability in each group was remained.

Secretome data analysis

To compare the secretomes from cell lines with different metastasis properties, the spectral counts of each cell line were normalized and the protein fold changes in two cell line groups were calculated as previously described. The cutoffs of fold changes ~ 2 and Student's *t*-test $P \sim 0.05$ were used to select the bone metastasis associated proteins.

The subcellular localizations of identified proteins were classified as secreted (predicted secreted), plasma membrane and intracellular. A protein was classified as secreted if it was designated as "extracellular" by the GO term, or as "secreted" in the UniProt database (http://www.uniprot.org/), or predicted as so by SignalP 3.0 (probability ~ 0.90) or SecretomeP 2.0 (NN-score ~ 0.50). A protein was classified as plasma membrane with its GO designation of "plasma membrane", or UniProt description of "cell membrane", or predicted by TMHMM 2.0 (http://www.cbs.dtu.dk/services/TMHMM/). Intracellular proteins were identified via their GO and UniProt designation. Unknown proteins were those that could not be classified by above sources.

Gene Ontology analysis of the biological processes and molecular functions were performed with the tool GOEAST (http://omicslab.genetics.ac.cn/GOEAST/index.php).

Immunoblot analysis of secreted proteins

To precipitate secreted proteins, 0.5 ml of 40% trichloroacetic acid was added to 0.5 ml CM. After incubation on ice for 1 h, the

samples were spun at 14 000× *g* for 30 min and the supernatants were discarded. Pellets were washed twice by spinning at 14 000× *g* for 5 min in cold acetone and re-suspended in SDS loading buffer. The proteins were separated by 15% SDS-PAGE and transferred onto a polyvinylidene filter using Mini Trans-Blot (Bio-Rad Laboratories). The filter was stained with Ponceau S and blocked by 5% nonfat milk in Tris-buffered saline with 0.1% Tween 20 for 1 h at room temperature. The filter was then incubated with a primary antibody overnight and washed, followed by blotting with a secondary antibody conjugated with HRP for 1 h. The signals were visualized with chemiluminescent HRP substrate (Millipore).

MSP and bisulfite sequencing

One μg of extracted DNA was modified with sodium bisulfite using the EZ DNA Methylation Gold Kit (ZYMO) according to the manufacturer's instructions. The CST6 primers for the methylation-specific reaction were 5′-TGGTCGGTATTAAGTATTTTTTGAC-3′ (sense) and 5′- AACCCAACTATTACCTCCTACTACG-3′ (antisense), and those for the unmethylation-specific reaction were 5′-GTTGGTATTAAGTATTTTTTGATGA-3′ (sense) and 5′- AACCCAACTATTACCTCCTACTACAC-3′ (antisense). For bisulfite sequencing, the fragment covering the CpG island of CST6 promoter was amplified from bisulfite-modified genomic DNA with primers 5′- GGAAATGGTGGTAATAGTAAGAGTTTA-3′ (sense) and 5′- AAATTCAAAAAACCCAAAAAACC-3′ (antisense). The PCR products were cloned into pcDNA3 vector, and 8-10 clones of each sample were sequenced.

Colony formation assay

Cells were suspended in DMEM containing 0.3% agarose gel (Invitrogen) at a concentration of 2×10^3 cells/ml. The suspension was seeded in a plate coated with 0.6% solidified agarose. The cells were incubated for 4 weeks before the colonies were counted and photographed with a Leica microscope.

Wound-healing assay

Cells were grown into confluence in 6-well plates. The monolayer was artificially injured by scratching across the plate with a 200-μl pipette tip. The wells were washed 3 times to remove detached cells or cell debris. After 12 h, images of the scratched areas were photographed. Scratch wound areas were measured and the migration distances were calculated as initial wound size - final wound size.

In vitro migration and invasion assays

Migration assays were conducted using transwells with polycarbonate membrane filters of 8-μm pore sizes (Costar, Cambridge, MA) in 24-well culture plates. For invasion assay, the upper chamber was coated with 40 μl Matrigel (Becton Dickinson, Bedford, MA). After being starved in FBS-free medium overnight, the cells were seeded in the upper chamber at a density of 10^5 cells per well. FBS was used in the lower chamber as the attractant. Cells that migrated or invaded into the lower surface were counted 24-48 h later. Random fields were photographed after crystal violet staining. Experiments were performed at least in triplicates.

For CM migration analysis, the serum-free CM from various cell lines were used in the upper and lower chamber of the transwell, and FBS was added into the lower chamber as the attractant.

Proteinase enzymatic activity assay

Cathepsin B (BioVision, K140-100) and cathepsin L (BioVision, K142-100) assays were performed with the activity assay kits according the manufacturer's instructions in 96-well plates. The assays were measured with a fluorometer (TECAN Safire 2, USA) equipped with a 400-nm excitation filter and a 505-nm emission filter. The CTSB inhibitor (CA-074, Merck) and the CTSL inhibitor (Z-FY[t-Bu]-DMK, Merck) were used as controls. The substrate Z-Ala-Ala-Asn-AMC (I1865, Bachem) was used for legumain activity assay with a 353-nm excitation filter and a 442-nm emission filter.

Animal studies

All animal experiments were performed in compliance with the guidelines for the care and use of laboratory animals and were approved by the institutional biomedical research ethics committee of Shanghai Institutes for Biological Sciences, Chinese Academy of Sciences. Female Balb/c nude mice (4-6 weeks old) were used in all animal studies.

To study primary tumor growth, cells were harvested by trypsinization, washed twice in PBS and counted. Cells were then resuspended (1×10^7 cells/ml) in 1:1 mixture of PBS and Matrigel. Mice were anaesthetized by 1% Pelltobarbitalum Natricum. A small incision was made to reveal the 4th mammary fat pad and 10^5 cells (10 μl) were injected directly into the fat pad. The incision was closed and tumor growth was monitored weekly by measuring the tumor length (L) and width (W). Tumor volumes were calculated as $\pi LW^2/6$.

For bone metastasis studies, 10^5 tumor cells in PBS (100 μl) were injected into the left cardiac ventricle of anesthetized mice. At each week, the anesthetized mice were retro-orbitally injected with 75 mg/kg D-Luciferin (Caliper Life Sciences), and BLI data was acquired with a Berthold NC100 Imaging System. Bone damages were monitored by X-ray radiography. Mice were anesthetized, arranged in prone position on single-wrapped films (X-OMAT Kodak) and exposed at 24 kV for 180 s with a Faxitron instrument (Faxitron Bioptics). Films were developed using a Konica SRX-101A processor and inspected for visible bone lesions. Osteolytic areas were identified on radiographs as demarcated radiolucent lesions in the bone and quantified using the Image J software (NIH).

Histological analysis and TRAP staining

Forelimb and hindlimb long bones of nude mice were excised, fixed in 10% neutral-buffered formalin, decalcified (10% EDTA, 2 weeks), dehydrated through a graded alcohol series, then embedded in paraffin and stained with hematoxylin and eosin.

TRAP staining was performed with the tartrate-resistant acid phosphatase kit (Sigma 387A). Osteoclast numbers were assessed as multinucleated TRAP+ cells along the tumor-bone interface and reported as number/mm of interface.

Statistical analysis

Results are presented as average ± standard deviation in the figures. Student's *t*-test was used to compare the *in vitro* data. Two-sided Wilcoxon rank test was performed to analyze the BLI data. Tumor volume and BLI growth curves were compared by re-

peated measures of ANOVA analysis. The Kaplan-Meier method was used to estimate survival curves for animals. Log-rank test were used to compare the animal survival.

Acknowledgments

We thank Dr Mario Blanco and Dr Yibin Kang at Princeton University for their assistance in cystatin overexpression plasmids. This work was supported by the National Basic Research Program of China (973 program; 2011CB510105, 2010CB834300), the National Natural Science Foundation of China (81071754, 81071792), Chinese Academy of Sciences (2009OHTP08, KSCX2-YW-R-192) and the Shanghai Pujiang Plan (10PJ1411600).

References

1 Jemal A, Bray F, Center MM, *et al.* Global cancer statistics. *CA Cancer J Clin* 2011; **61**:69-90.
2 Hess KR, Varadhachary GR, Taylor SH, *et al.* Metastatic patterns in adenocarcinoma. *Cancer* 2006; **106**:1624-1633.
3 Mundy GR. Metastasis to bone: causes, consequences and therapeutic opportunities. *Nat Rev Cancer* 2002; **2**:584-593.
4 Suva LJ, Washam C, Nicholas RW, Griffin RJ. Bone metastasis: mechanisms and therapeutic opportunities. *Nat Rev Endocrinol* 2011; **7**:208-218.
5 Xue H, Lu B, Lai M. The cancer secretome: a reservoir of biomarkers. *J Transl Med* 2008; **6**:52.
6 Langley RR, Fidler IJ. The seed and soil hypothesis revisited--the role of tumor-stroma interactions in metastasis to different organs. *Int J Cancer* 2011; **128**:2527-2535.
7 Muller A, Homey B, Soto H, *et al.* Involvement of chemokine receptors in breast cancer metastasis. *Nature* 2001; **410**:50-56.
8 Condeelis J, Pollard JW. Macrophages: obligate partners for tumor cell migration, invasion, and metastasis. *Cell* 2006; **124**:263-266.
9 Egeblad M, Werb Z. New functions for the matrix metalloproteinases in cancer progression. *Nat Rev Cancer* 2002; **2**:161-174.
10 Nomura T, Katunuma N. Involvement of cathepsins in the invasion, metastasis and proliferation of cancer cells. *J Med Invest* 2005; **52**:1-9.
11 Yang SY, Miah A, Pabari A, Winslet M. Growth Factors and their receptors in cancer metastases. *Front Biosci* 2011; **16**:531-538.
12 Kaplan RN, Riba RD, Zacharoulis S, *et al.* VEGFR1-positive haematopoietic bone marrow progenitors initiate the pre-metastatic niche. *Nature* 2005; **438**:820-827.
13 Caccia D, Zanetti Domingues L, Micciche F, *et al.* Secretome compartment is a valuable source of biomarkers for cancer-relevant pathways. *J Proteome Res* 2011; **10**:4196-4207.
14 Zhong L, Roybal J, Chaerkady R, *et al.* Identification of secreted proteins that mediate cell-cell interactions in an in vitro model of the lung cancer microenvironment. *Cancer Res* 2008; **68**:7237-7245.
15 Kashyap MK, Harsha HC, Renuse S, *et al.* SILAC-based quantitative proteomic approach to identify potential biomarkers from the esophageal squamous cell carcinoma secretome. *Cancer Biol Ther* 2010; **10**:796-810.
16 Gronborg M, Kristiansen TZ, Iwahori A, *et al.* Biomarker discovery from pancreatic cancer secretome using a differential proteomic approach. *Mol Cell Proteomics* 2006; **5**:157-171.
17 Wu CC, Hsu CW, Chen CD, *et al.* Candidate serological biomarkers for cancer identified from the secretomes of 23 cancer cell lines and the human protein atlas. *Mol Cell Proteomics* 2010; **9**:1100-1117.
18 Weng LP, Wu CC, Hsu BL, *et al.* Secretome-based identification of Mac-2 binding protein as a potential oral cancer marker involved in cell growth and motility. *J Proteome Res* 2008; **7**:3765-3775.
19 Ohanna M, Giuliano S, Bonet C, *et al.* Senescent cells develop a PARP-1 and nuclear factor-{kappa}B-associated secretome (PNAS). *Genes Dev* 2011; **25**:1245-1261.
20 Chang YT, Wu CC, Shyr YM, *et al.* Secretome-based identification of ULBP2 as a novel serum marker for pancreatic cancer detection. *PLoS One* 2011; **6**:e20029.
21 Kreunin P, Urquidi V, Lubman DM, Goodison S. Identification of metastasis-associated proteins in a human tumor metastasis model using the mass-mapping technique. *Proteomics* 2004; **4**:2754-2765.
22 Rocco M, Malorni L, Cozzolino R, *et al.* Proteomic profiling of human melanoma metastatic cell line secretomes. *J Proteome Res* 2011; **10**:4703-4714.
23 Mbeunkui F, Metge BJ, Shevde LA, Pannell LK. Identification of differentially secreted biomarkers using LC-MS/MS in isogenic cell lines representing a progression of breast cancer. *J Proteome Res* 2007; **6**:2993-3002.
24 Xue H, Lu B, Zhang J, *et al.* Identification of serum biomarkers for colorectal cancer metastasis using a differential secretome approach. *J Proteome Res* 2010; **9**:545-555.
25 Wang CL, Wang CI, Liao PC, *et al.* Discovery of retinoblastoma-associated binding protein 46 as a novel prognostic marker for distant metastasis in nonsmall cell lung cancer by combined analysis of cancer cell secretome and pleural effusion proteome. *J Proteome Res* 2009; **8**:4428-4440.
26 Chiu KH, Chang YH, Wu YS, Lee SH, Liao PC. Quantitative secretome analysis reveals that COL6A1 is a metastasis-associated protein using stacking gel-aided purification combined with iTRAQ labeling. *J Proteome Res* 2011; **10**:1110-1125.
27 Ween MP, Lokman NA, Hoffmann P, *et al.* Transforming growth factor-beta-induced protein secreted by peritoneal cells increases the metastatic potential of ovarian cancer cells. *Int J Cancer* 2011; **128**:1570-1584.
28 Rondepierre F, Bouchon B, Bonnet M, *et al.* B16 melanoma secretomes and in vitro invasiveness: syntenin as an invasion modulator. *Melanoma Res* 2010; **20**:77-84.
29 Kang Y, Siegel PM, Shu W, *et al.* A multigenic program mediating breast cancer metastasis to bone. *Cancer Cell* 2003; **3**:537-549.
30 Korpal M, Yan J, Lu X, *et al.* Imaging transforming growth factor-beta signaling dynamics and therapeutic response in breast cancer bone metastasis. *Nat Med* 2009; **15**:960-966.
31 Sethi N, Dai X, Winter CG, Kang Y. Tumor-derived JAGGED1 promotes osteolytic bone metastasis of breast cancer by engaging notch signaling in bone cells. *Cancer Cell* 2011; **19**:192-205.
32 Serganova I, Moroz E, Vider J, *et al.* Multimodality imaging of TGFbeta signaling in breast cancer metastases. *FASEB J*

2009; **23**:2662-2672.
33 Minn AJ, Kang Y, Serganova I, *et al.* Distinct organ-specific metastatic potential of individual breast cancer cells and primary tumors. *J Clin Invest* 2005; **115**:44-55.
34 Ganapathy V, Ge R, Grazioli A, *et al.* Targeting the Transforming Growth Factor-beta pathway inhibits human basal-like breast cancer metastasis. *Mol Cancer* 2010; **9**:122.
35 Subramanian A, Tamayo P, Mootha VK, *et al.* Gene set enrichment analysis: a knowledge-based approach for interpreting genome-wide expression profiles. *Proc Natl Acad Sci USA* 2005; **102**:15545-15550.
36 Ochieng J, Chaudhuri G. Cystatin superfamily. *J Health Care Poor Underserved* 2010; **21(1 Suppl)**:51-70.
37 Lu X, Mu E, Wei Y, *et al.* VCAM-1 Promotes Osteolytic Expansion of Indolent Bone Micrometastasis of Breast Cancer by Engaging alpha4beta1-Positive Osteoclast Progenitors. *Cancer Cell* 2011; **20**:701-714.
38 Ai L, Kim WJ, Kim TY, *et al.* Epigenetic silencing of the tumor suppressor cystatin M occurs during breast cancer progression. *Cancer Res* 2006; **66**:7899-7909.
39 Rivenbark AG, Jones WD, Coleman WB. DNA methylation-dependent silencing of CST6 in human breast cancer cell lines. *Lab Invest* 2006; **86**:1233-1242.
40 Gyorffy B, Lanczky A, Eklund AC, *et al.* An online survival analysis tool to rapidly assess the effect of 22,277 genes on breast cancer prognosis using microarray data of 1,809 patients. *Breast Cancer Res Treat* 2010; **123**:725-731.
41 Zhang XH, Wang Q, Gerald W, *et al.* Latent bone metastasis in breast cancer tied to Src-dependent survival signals. *Cancer Cell* 2009; **16**:67-78.
42 Zhang J, Shridhar R, Dai Q, *et al.* Cystatin m: a novel candidate tumor suppressor gene for breast cancer. *Cancer Res* 2004; **64**:6957-6964.
43 Rivenbark AG, Livasy CA, Boyd CE, Keppler D, Coleman WB. Methylation-dependent silencing of CST6 in primary human breast tumors and metastatic lesions. *Exp Mol Pathol* 2007; **83**:188-197.
44 Cheng T, van Vlijmen-Willems IM, Hitomi K, *et al.* Colocalization of cystatin M/E and its target proteases suggests a role in terminal differentiation of human hair follicle and nail. *J Invest Dermatol* 2009; **129**:1232-1242.
45 Sotiropoulou G, Anisowicz A, Sager R. Identification, cloning, and characterization of cystatin M, a novel cysteine proteinase inhibitor, down-regulated in breast cancer. *J Biol Chem* 1997; **272**:903-910.
46 Minn AJ, Gupta GP, Siegel PM, *et al.* Genes that mediate breast cancer metastasis to lung. *Nature* 2005; **436**:518-524.
47 Bos PD, Zhang XH, Nadal C, *et al.* Genes that mediate breast cancer metastasis to the brain. *Nature* 2009; **459**:1005-1009.
48 Lu X, Wang Q, Hu G, *et al.* ADAMTS1 and MMP1 proteolytically engage EGF-like ligands in an osteolytic signaling cascade for bone metastasis. *Genes Dev* 2009; **23**:1882-1894.
49 Giles ED, Singh G. Role of insulin-like growth factor binding proteins (IGFBPs) in breast cancer proliferation and metastasis. *Clin Exp Metastasis* 2003; **20**:481-487.
50 Ye L, Bokobza SM, Jiang WG. Bone morphogenetic proteins in development and progression of breast cancer and therapeutic potential (review). *Int J Mol Med* 2009; **24**:591-597.
51 Shen Y, Winkler IG, Barbier V, *et al.* Tissue inhibitor of metalloproteinase-3 (TIMP-3) regulates hematopoiesis and bone formation *in vivo*. *PLoS One* 2010; **5**:e13086.
52 Yoon KJ, Phelps DA, Bush RA, *et al.* ICAM-2 expression mediates a membrane-actin link, confers a nonmetastatic phenotype and reflects favorable tumor stage or histology in neuroblastoma. *PLoS One* 2008; **3**:e3629.
53 Koblinski JE, Ahram M, Sloane BF. Unraveling the role of proteases in cancer. *Clin Chim Acta* 2000; **291**:113-135.
54 Tseng MY, Liu SY, Chen HR, *et al.* Serine protease inhibitor (SERPIN) B1 promotes oral cancer cell motility and is over-expressed in invasive oral squamous cell carcinoma. *Oral Oncol* 2009; **45**:771-776.
55 Krepela E, Prochazka J, Karova B, Cermak J, Roubkova H. Cysteine proteases and cysteine protease inhibitors in non-small cell lung cancer. *Neoplasma* 1998; **45**:318-331.
56 Coussens LM, Fingleton B, Matrisian LM. Matrix metalloproteinase inhibitors and cancer: trials and tribulations. *Science* 2002; **295**:2387-2392.
57 Bialas A, Kafarski P. Proteases as anti-cancer targets--molecular and biological basis for development of inhibitor-like drugs against cancer. *Anticancer Agents Med Chem* 2009; **9**:728-762.
58 Zeeuwen PL, van Vlijmen-Willems IM, Cheng T, *et al.* The cystatin M/E-cathepsin L balance is essential for tissue homeostasis in epidermis, hair follicles, and cornea. *FASEB J* 2010; **24**:3744-3755.
59 Zeeuwen PL, van Vlijmen-Willems IM, Hendriks W, Merkx GF, Schalkwijk J. A null mutation in the cystatin M/E gene of ichq mice causes juvenile lethality and defects in epidermal cornification. *Hum Mol Genet* 2002; **11**:2867-2875.
60 Pulukuri SM, Gorantla B, Knost JA, Rao JS. Frequent loss of cystatin E/M expression implicated in the progression of prostate cancer. *Oncogene* 2009; **28**:2829-2838.
61 Kim TY, Zhong S, Fields CR, Kim JH, Robertson KD. Epigenomic profiling reveals novel and frequent targets of aberrant DNA methylation-mediated silencing in malignant glioma. *Cancer Res* 2006; **66**:7490-7501.
62 Veena MS, Lee G, Keppler D, *et al.* Inactivation of the cystatin E/M tumor suppressor gene in cervical cancer. *Genes Chromosomes Cancer* 2008; **47**:740-754.
63 Morris MR, Ricketts C, Gentle D, *et al.* Identification of candidate tumour suppressor genes frequently methylated in renal cell carcinoma. *Oncogene* 2010; **29**:2104-2117.
64 Vigneswaran N, Wu J, Nagaraj N, *et al.* Silencing of cystatin M in metastatic oral cancer cell line MDA-686Ln by siRNA increases cysteine proteinases and legumain activities, cell proliferation and in vitro invasion. *Life Sci* 2006; **78**:898-907.
65 Briggs JJ, Haugen MH, Johansen HT, *et al.* Cystatin E/M suppresses legumain activity and invasion of human melanoma. *BMC Cancer* 2010; **10**:17.
66 Keppler D. Towards novel anti-cancer strategies based on cystatin function. *Cancer Lett* 2006; **235**:159-176.
67 Ross DT, Scherf U, Eisen MB, *et al.* Systematic variation in gene expression patterns in human cancer cell lines. *Nat Genet* 2000; **24**:227-235.
68 Sellappan S, Grijalva R, Zhou X, *et al.* Lineage infidelity of MDA-MB-435 cells: expression of melanocyte proteins in a breast cancer cell line. *Cancer Res* 2004; **64**:3479-3485.
69 Rae JM, Ramus SJ, Waltham M, *et al.* Common origins of

MDA-MB-435 cells from various sources with those shown to have melanoma properties. *Clin Exp Metastasis* 2004; **21**:543-552.
70 Rae JM, Creighton CJ, Meck JM, Haddad BR, Johnson MD. MDA-MB-435 cells are derived from M14 melanoma cells--a loss for breast cancer, but a boon for melanoma research. *Breast Cancer Res Treat* 2007; **104**:13-19.
71 Chambers AF. MDA-MB-435 and M14 cell lines: identical but not M14 melanoma? *Cancer Res* 2009; **69**:5292-5293.
72 Rawlings ND, Barrett AJ, Bateman A. MEROPS: the peptidase database. *Nucleic Acids Res* 2010; **38** (Database issue):D227-233.
73 Yao L, Zhang Y, Chen K, Hu X, Xu LX. Discovery of IL-18 As a Novel Secreted Protein Contributing to Doxorubicin Resistance by Comparative Secretome Analysis of MCF-7 and MCF-7/Dox. *PLoS One* 2011; **6**:e24684.
74 Bendtsen JD, Nielsen H, von Heijne G, Brunak S. Improved prediction of signal peptides: SignalP 3.0. *J Mol Biol* 2004; **340**:783-795.
75 Bendtsen JD, Jensen LJ, Blom N, Von Heijne G, Brunak S. Feature-based prediction of non-classical and leaderless protein secretion. *Protein Eng Des Sel* 2004; **17**:349-356.

(**Supplementary information** is linked to the online version of the paper on the *Cell Research* website.)